

Unsupervised Real-to-Virtual Domain Unification for End-to-End Highway Driving

Luona Yang¹ Xiaodan Liang^{1,2} Eric P. Xing²
 Carnegie Mellon University¹ Petuum Inc.²

Abstract

In the spectrum of vision-based autonomous driving, vanilla end-to-end models are not interpretable and suboptimal in performance, while mediated perception models require additional intermediate representations such as segmentation masks or detection bounding boxes, whose annotation can be prohibitively expensive as we move to a larger scale. Raw images and existing intermediate representations are also loaded with nuisance details that are irrelevant to the prediction of vehicle commands, e.g. the style of the car in front or the view beyond the road boundaries. More critically, all prior works fail to deal with the notorious domain shift if we were to merge data collected from different sources, which greatly hinders the model generalization ability. In this work, we address the above limitations by taking advantage of virtual data collected from driving simulators, and present DU-drive, an unsupervised real to virtual domain unification framework for end-to-end driving. It transforms real driving data to its canonical representation in the virtual domain, from which vehicle control commands are predicted. Our framework has several advantages: 1) it maps driving data collected from different source distributions into a unified domain, 2) it takes advantage of annotated virtual data which is free to obtain, 3) it learns an interpretable, canonical representation of driving image that is specialized for vehicle command prediction. Extensive experiments on two public highway driving datasets clearly demonstrate the performance superiority and interpretive capability of DU-drive.

1. Introduction

The development of a vision-based autonomous driving system has been a long-standing research problem [27, 24, 10, 9]. Of the various solutions that have been proposed, end-to-end driving models that map a single frontal camera image to vehicle control commands have attracted much research interest [5, 33, 18] as it eliminates the tedious process of feature engineering. Many attempts have also been made to improve the performance of vanilla end-to-

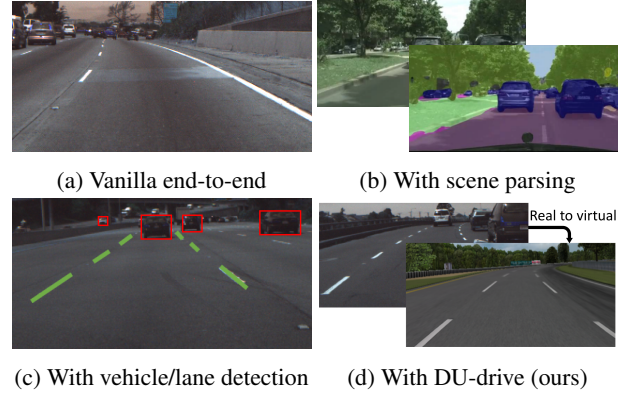


Figure 1: Various methods have been proposed for vision-based driving models. While vanilla end-to-end models (a) are not interpretable and suboptimal in performance, scene parsing (b) or object detection (c) requires expensively annotated data. Our method (d) unifies real images from different datasets into their canonical representations in the virtual domain that is free of superfluous details, which boosts the performance of vehicle command prediction task.

end models by taking advantage of intermediate representations (Figure 1). For example, [33] uses semantic segmentation as a side task to improve model performance, while [8] first trains a detector to detect nearby vehicles before making driving decisions. However, the collection of driving data and the annotation of intermediate representation can be prohibitively expensive as we move to a larger scale.

Moreover, general images and intermediate representations of driving scenes are loaded with superfluous details due to the complexity of the real world. Many of those details are nuisance information that is neither relevant nor helpful to the prediction task. For example, a typical human driver driving on a highway will not change her behavior according to the brand of the car in front, or the view beyond the road boundaries. Ideally, the model should be able to learn the critical information just by observing human driving data, but because of the black-box nature of deep neural networks, it is difficult to analyze whether the model has learned to make predictions based on the right

signals. [6] visualizes the activation of the neural network and shows that the model not only learns driving-critical information such as lane markings, but also unexpected features such as atypical vehicle classes. [18] presents results of attention map refined by causal filtering, which seems to include rather random attention blobs. It is difficult to justify that learning such information could be helpful to driving, and we believe that the ability to effectively distill the minimal sufficient information from driving images is critical to boosting the performance of the prediction task.

In contrast, driving data hooked from simulators naturally avoids both problems. On one hand, we can easily obtain unlimited driving data annotated with control signals by simply setting up a robot car. On the other hand, we can control the visual appearance of the virtual world and construct a canonical driving environment by keeping the superfluous details to a minimum.

This motivates us to develop a system that can effectively transform real driving images to their canonical representations in the virtual domain, and thus facilitate the vehicle command prediction task. Many existing works take advantage of virtual data by transforming virtual images to realistic looking images with generative adversarial network [12], while keeping the annotation intact with the help of auxiliary objectives [34, 7]. Our approach, while also based on GAN, is different in several aspects. First, we attempt to transform real images to their canonical representation in the virtual domain, instead of the other way around. By canonical representation, we refer to the pixel level representation that disentangles the minimum sufficient information for the prediction task from the background. Since any image can only have one canonical representation, we do not introduce any noise variable in the generation process. Second, we do not attempt to directly retain annotation as it is unclear what exact signals in the images determine the vehicle command. Instead, we propose a novel joint training scheme to gradually distill prediction critical information into the generator, which also stabilizes training and prevent mode collapse of driving critical information.

Our work has three novel contributions. First, we introduce an unsupervised real-to-virtual domain unification framework that transforms real driving images to their canonical representations in the virtual domain, from which vehicle commands are predicted. Second, we develop a novel training scheme that not only gradually distills prediction-critical information into the generator but also selectively prevents mode collapse of GAN. Third, we present experimental results that testify the superiority of using a unified, canonical representation in the virtual domain for end-to-end driving.

2. Related Work

2.1. Vision-based autonomous driving

Vision-based solutions are believed to be a promising direction for solving autonomous driving due to its low sensor cost and recent developments in computer vision. Since the first successful demonstration in the 1980s [27, 10, 9], various methods have been investigated in the spectrum of vision-based driving models, from end-to-end methods to full pipeline methods [16]. The ALVINN system[24], first introduced in 1989, is the pioneering work in end-to-end learning for autonomous driving. It shows that an end-to-end model can indeed learn to steer on simple road conditions. The network architecture has since evolved from the small fully-connected network of ALVINN into convolutional networks used by DAVE system[1] and then deep models used by DAVE-2 system[5]. Intermediate representations such as semantic segmentation masks and attention maps are shown to be helpful to improving the performance[33, 18].

Pipeline methods separate the parsing of the scene and the control of the vehicle. [8] first trains a vehicle detector to determine the location of adjacent cars and outputs vehicle commands according to a simple control logic. [14] shows that convolutional neural networks can be used to do lane and vehicle detection at a real-time frame rate. While such methods are more interpretable and controllable, the annotation of intermediate representations can be very expensive. Furthermore, runtime performance could also be compromised due to additional intermediate steps.

Our method takes advantage of an intermediate representation obtained from unsupervised training and therefore improves the performance of vanilla end-to-end driving models without introducing any annotation cost.

2.2. Domain Adaption for Visual Data

Ideally, a model trained for a specific task should be able to generalize to new datasets collected for the same task, yet research has shown that model performance could seriously degrade when input distribution changes due to the inherent bias introduced in the data collection process [29]. This phenomenon is known as domain shift or dataset bias. In the world of autonomous driving, it is even more critical to have a model that can generalize well to unseen scenarios.

Domain adaption methods attempt to battle domain shift by bridging the gap between the distribution of source data and target data [4, 23]. Recently, generative adversarial network (GAN) based domain adaption, also known as adversarial adaption, has achieved remarkable results in the field of visual domain adaption. [31] introduces a framework that subsumes several approaches as special cases [11, 30, 20]. It frames adversarial adaption as training an encoder (generator) that transforms data in the target domain to the source

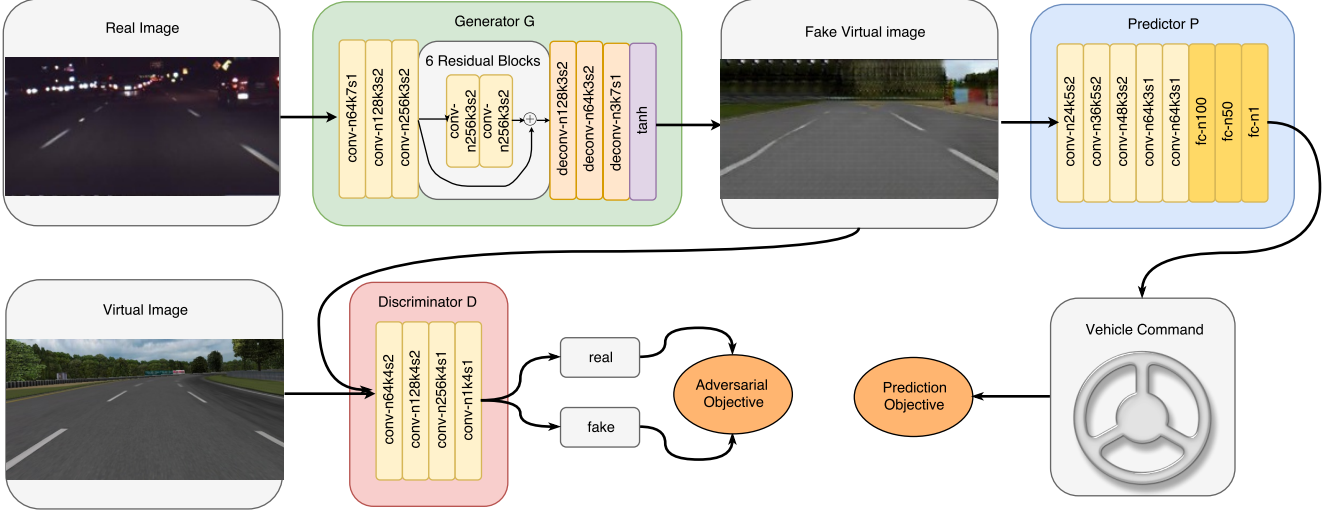


Figure 2: Model architecture for DU-Drive. The generator network G transforms input real image to fake virtual image, from which vehicle command is predicted by the predictor network P . The discriminator network D tries to distinguish the fake virtual images from true virtual images. Both the adversarial objective and the prediction objective drive the generator G to generate virtual representations that are most helpful to prediction task. For simplicity, instance normalization and activation layers after each convolutional/fully connected layer are omitted. (Abbr: n: number of filters, k: kernel size, s: stride size)

domain at a certain feature level trying to fool the adversarial discriminator, which in turn tries to distinguish the generated data from those sampled from the source domain. The line of work on style transfer [35, 15, 17] could also be potentially applied to domain adaption at the pixel level.

One subarea especially to our interest is the adaption of virtual data to real data. As the collection of real-world data can be excessively expensive in certain cases, virtual data rendered with computer graphics technologies can come to remedy if we could adapt knowledge learned in the virtual domain to the real domain. [7] proposed a GAN-based model that transforms data from virtual domain to the real domain in the pixel space in an unsupervised manner by utilizing a content-similarity loss to retain annotation. [26] uses adversarial training to improve the realism of synthetic images with the help a self-regularization term, a local adversarial loss and a buffer of training images for the discriminator. [28] randomizes the texture of objects in the robot simulator and trains a visuomotor policy without using any real-world data. [34] trains a driving policy with reinforcement learning in a simulator by transforming virtual images to real images, retaining the scene structure with adversarial loss on the segmentation mask.

While existing work aims at transforming virtual images to realistic looking images, we argue that doing the other way around could be more advantageous for learning a driving policy. The transformation from real to virtual is an easier task as it is more manageable to go from complex to simple, and all real datasets could be unified into their canonical representations in the virtual domain where nuisance details are eliminated.

3. Unsupervised Domain Unification

We first introduce the overall design of our framework (Figure 2), then dive into the details of the learning process.

3.1. Network design and learning objective

Learning Objective for DU-Drive Given a dataset of driving images labeled with vehicle command in the real domain and a similar dataset in the virtual domain, our goal is to transform a real image to its canonical form in the virtual domain and then run prediction algorithm on the transformed fake virtual image. Our model is closely related to conditional GAN [22], where the generator and discriminator both takes a conditional factor as input, yet different in two subtle aspects. One is that in our model, the discriminator does not depend on the conditional factor. The other is that our generator does not take any noise vector as input. Unlike the mapping from a plain virtual image to a rich real image, where there could be multiple feasible solutions, the mapping from a real image to its canonical form that contains only the minimal sufficient information for the prediction task should be unique. Therefore, we could remove the noise term in conventional GANs and use a deterministic generative network as our generator.

More formally, let $\mathbf{X}^r = \{\mathbf{x}_i^r, \mathbf{y}_i^r\}_{i=1}^{N_r}$ be a labeled dataset with N^r samples in the real domain, and let $\mathbf{X}^v = \{\mathbf{x}_i^v, \mathbf{y}_i^v\}_{i=1}^{N^v}$ be a labeled dataset with N^v samples in the virtual domain, where \mathbf{x} is the frontal image of a driving scene and \mathbf{y} is the corresponding vehicle command. Our DU-drive model consists of a deterministic conditional generator $G(\mathbf{x}^r; \theta_G) \rightarrow \mathbf{x}^f$, parametrized by θ_G , that maps an

image $\mathbf{x}^r \in \mathbf{X}^r$ in the real domain to a fake virtual image \mathbf{x}^f , a virtual discriminator $D(\mathbf{x}^v; \theta_D)$ that discriminates whether a image is sampled from true virtual images or from fake virtual images, and a predictor $P(\mathbf{x}^v; \theta_P) \rightarrow y^v$, that maps a virtual image to a vehicle control command.

The learning objective of DU-drive is:

$$\min_{\theta_G, \theta_P} \max_{\theta_D} \mathcal{L}_d(D, G) + \lambda L_t(P, G), \quad (1)$$

where $\mathcal{L}_d(D, G)$ is the domain loss, which the generator tries to minimize and the discriminator tries to maximize in the minimax game of GAN. $\mathcal{L}_d(D, G)$ is defined as:

$$\mathcal{L}_d(D, G) = \mathbb{E}_{\mathbf{x}^v} [\log D(\mathbf{x}^v; \theta_D)] + \mathbb{E}_{\mathbf{x}^r} [\log(1 - D(G(\mathbf{x}^r; \theta_G); \theta_D))], \quad (2)$$

$\mathcal{L}_t(P, G)$ is the task specific objective for predictor and generator, which in this work is the mean square loss between the predicted control command and the ground truth control command, defined as:

$$\mathcal{L}_t(P, G) = \mathbb{E}_{\mathbf{x}^r} [\|P(G(\mathbf{x}^r; \theta_G), \theta_P) - \mathbf{y}^r\|_2^2] \quad (3)$$

λ is a hyperparameter that controls the weight of task-specific loss and the domain loss.

Network Design For the GAN part of the model, we mostly adopt the network architecture as defined in [17], which has achieved impressive results in style transfer task. The generator network consists of two convolutional layers with 3x3 kernel and stride size 2, followed by 6 residual blocks. Two deconvolutional layers with stride 1/2 then transform the feature to the same size as the input image. We use instance normalization for all the layers. For the discriminator network, we use a fully convolutional network with convolutional layers of filter size 64, 128, 256 and 1 respectively. Each convolutional layer is followed by instance normalization and Leaky ReLU nonlinearity. We do not use PatchGAN as employed in [15] because driving command prediction needs global structure information.

For the predictor network, we adopt the network architecture used in DAVE-2 system[5], also known as *Pilot-Net*, as it has achieved decent results in end-to-end driving [17, 6, 5]. The network contains 5 convolutional layers and 4 fully connected layers. The first three convolutional layers have kernel size 5x5 and stride size 3, while the last two layers have kernel size 3x3 and stride size 1. No padding is used. The last convolutional layer is flattened and immediately followed by four fully connected layers with output size 100, 50, 10 and 1 respectively. All layers use ReLU activation.

3.2. Learning

Our goal is to learn a conditional generator that maps a real image to its canonical representation in the virtual domain. However, a naive application of conditional GAN

is insufficient for two reasons. First, the adversarial loss only provides supervision at the level of image distribution and does not guarantee the retention of the label after transformation. Second, conventional GANs are vulnerable to mode collapse, a common pitfall during the optimization of the GAN objective where the distribution of transformed images degenerates. Previous work on adapting virtual image to real image alleviates those problems by introducing a task-specific loss to add further constraint to the image generated. For example, [7] uses a content similarity loss to enforce that the foreground of the generated image matches with that of the input image. [26] employs a self-regularization term that minimizes the image difference between the synthetic and refined images.

Unfortunately, we cannot take advantage of similar techniques as the "foreground", or the information critical to retaining the label is not obvious for autonomous driving. Instead, we introduce a progressive training scheme when training the conditional generator, where the supervision from the prediction task gradually drives the generator to convert the input images from the real domain to its corresponding representation in the virtual domain that is most suitable for the prediction task. More formally, our objective in Equation 1 can be decomposed into three parts with respect to the three networks G , P and D :

$$\min_{\theta_G} \mathcal{L}_d(D, G) + \lambda L_t(P, G), \quad (4)$$

$$\min_{\theta_P} L_t(P, G), \quad (5)$$

$$\max_{\theta_D} \mathcal{L}_d(D, G) \quad (6)$$

We omit the weight term λ in Equation 6, as it is easy to see that only θ_G is influenced by both the domain loss and the prediction loss, and we can train θ_D , θ_G and θ_P with respect to the three objectives above independently. We denote α_P as the learning rate for updating θ_P , and α_{GAN} as the learning rate for updating θ_D and θ_G .

During training, we update θ_D , θ_G and θ_P sequentially by optimizing the above three objectives, so that the generation quality and prediction performance improves hand in hand. We first set $\lambda = 0$, and then increase it progressively, so that the weight of the task-specific loss won't go up too quickly at an early stage that it disturbs the equilibrium established between the generator and the discriminator.

3.3. Domain Unification

Consider the case when we have multiple real datasets $\{\mathbf{x}^{r_1}, \mathbf{y}^{r_1}\}, \dots, \{\mathbf{x}^{r_n}, \mathbf{y}^{r_n}\}$. Due to different data distribution depicted by road appearance, lighting conditions or driving scenes, each dataset belongs to a unique domain which we denote as D_{r_1}, \dots, D_{r_n} respectively. Prior works on end-to-end driving tend to deal with only one domain rather than a more general reasoning system. DU-drive, however, unifies

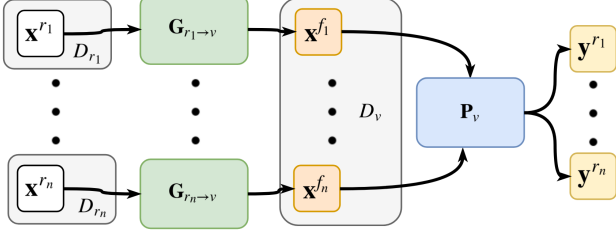


Figure 3: Domain unification by DU-drive. For each real domain, a generator is trained independently to transform real images to fake virtual images in a unified virtual domain. A single virtual image to vehicle command predictor is trained to do prediction across multiple real domains.

data from different real domains into a single virtual domain and eliminates the notorious domain shift problem.

For each real domain D_{r_i} , we use our DU-drive model to train a generator that transforms images \mathbf{x}^{r_i} into their canonical representations \mathbf{x}^{f_i} in a unified virtual domain D_v (Figure 3). A global predictor P_v could then be trained to do vehicle command prediction from the transformed virtual images. We fix the generator for each real domain and train the global predictor with labeled data from multiple real domains simultaneously. Same as our training setup for a single domain, we also use *PilotNet* pretrained on virtual data as our initialization for the global predictor.

4. Experiments

4.1. Data

We use TORCS[32], an open-source car racing simulator, as our platform for virtual data collection. We set up our environment in a minimalist way, with only clearly painted lane markings and toy-style traffic cars on the road. Figure 4 shows some images randomly sampled from the datasets. We construct a virtual dataset with over thirty thousand frames of driving data. A robot car that follows a simple driving policy as defined in [8] is set up as our host car, from which virtual frontal camera images and steering commands are captured. We also included twelve traffic cars that follow a simple control logic as defined in [8], with random noise added to the control commands to encourage varied behaviors. We captured our data on six game tracks with different shapes, which are summarized in Figure 6. We keep the lane settings uniform across all tracks, *i.e.* with three equally spaced lanes where the robot cars run on, as we believe this could serve as a canonical driving environment. To account for the imbalance of right turns and left turns in the virtual data, which could introduce bias in the domain transformation process, we augment our data by flipping the image and negate the steering command.

We use two large-scale real-world datasets released by Comma.ai[25] and Udacity[2] respectively (Table 1). Both datasets are composed of several episodes of high-way

driving videos. The Comma.ai dataset contains 9 training episodes and 2 testing episodes. Three of the training episodes and one of the testing episodes are captured at night, while others are captured during the daytime. We follow the data reader provided by [25] and filter out data points where the steering wheel angle is greater than 200. Good consistency could be observed for lighting/road conditions and roadside views. For Udacity dataset, we use the official release of training/testing data for challenge II at [2]. A relatively larger variance could be observed for lighting/road conditions and roadside views.

Dataset	train/test frames	Lighting	size
Comma.ai	345887/32018	Day/Night	160 x 320
Udacity	33808/5279	Day	240 x 320
TORCS	30183/3354	Day	240 x 320

Table 1: Dataset details.

4.2. Preprocessing

We first crop the input image to 160 x 320 by removing the extra upper part, which is usually background sky that does not change driving behavior. We then resize the image to 80 x 320 and normalize the pixel values to [-1, 1].

We focus on the prediction of steering angle in this work, though extensions to other vehicle commands should not be difficult. Instead of predicting the steering angle command directly, we predict the inverse of the radius as it is more stable and invariant to the geometry of the data capturing car [18, 5]. The relationship between the inverse turning radius u_t and steering angle θ_t is characterized by Ackermann steering geometry as:

$$\theta_t = u_t d_w K_s (1 + K_{slip} v_t^2) \quad (8)$$

where θ_t is the steering command in radius, $u_t(1/m)$ is the inverse of the turning radius, $v_t(m/s)$ is the vehicle speed at time t . $d_w(m)$ stands for the wheelbase, which is the distance between the front and the rear wheel. K_{slip} is the slippery coefficient. K_s is the steering ratio between the turn of the steer and the turn of the wheels. We get d_w and K_s from car specifics released by the respective car manufacturer of the data capturing vehicle, and use the K_{slip} provided by Comma.ai [25], which is estimated from real data. After predicting u_t , we transform it back to θ_t according to equation 8 and measure the mean absolute error of steering angle prediction.

4.3. Training details

All the models are implemented in Tensorflow [3] and trained on an NVIDIA Titan-X GPU. We train all networks with Adam optimizer [19] and set $\beta_1 = 0.5$. We follow the techniques used in [35] to stabilize the training. First, we use LSGAN [21], where the conventional GAN objective is replaced by a least square loss. Thus the loss function

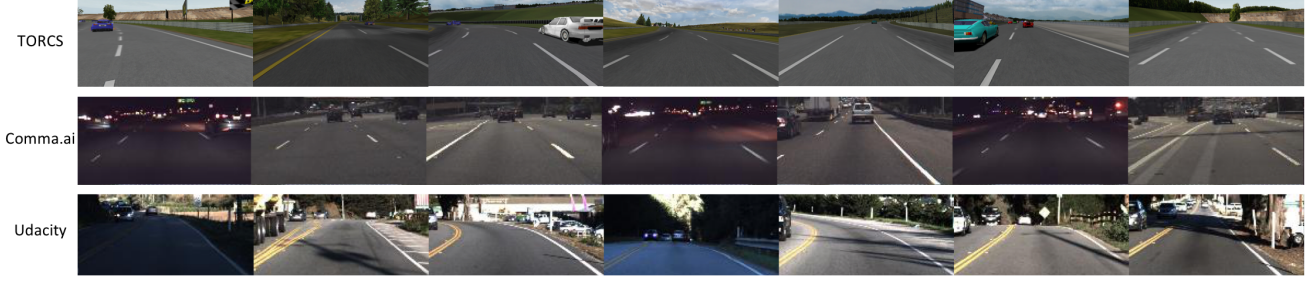


Figure 4: Sample data used by our work. From top to down: Virtual data captured from TORCS simulator, real driving data from comma.ai, real driving data from Udacity Challenge.

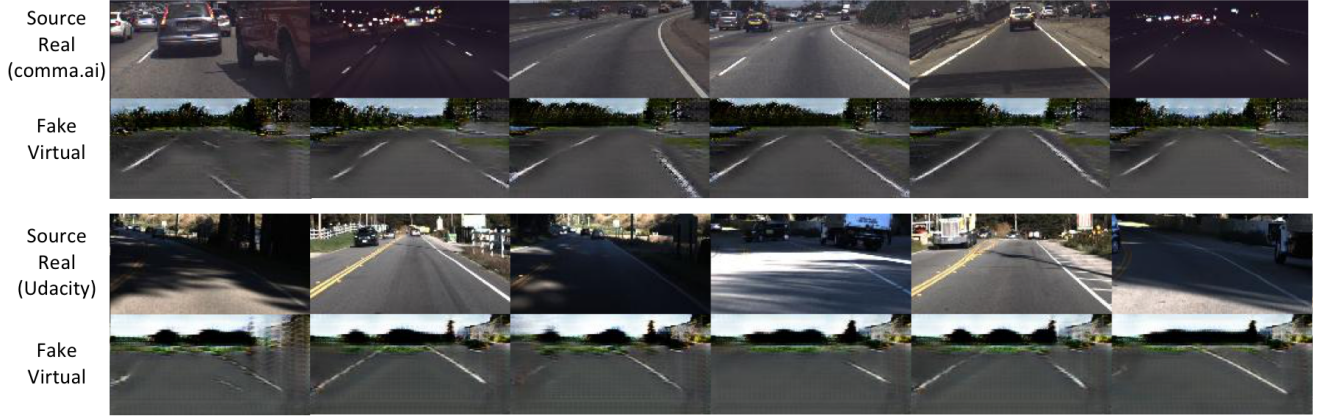


Figure 5: Image generation results of DU-Drive. Observe that information not critical to driving behavior, *e.g.* day/night lighting condition and view beyond road boundary, is unified. Interestingly, vehicles are also removed from the scenes, which is actually reasonable on second thought considering that we are only predicting steering angles in our experiments. On the other hand, driving critical information like lane markings are well preserved.

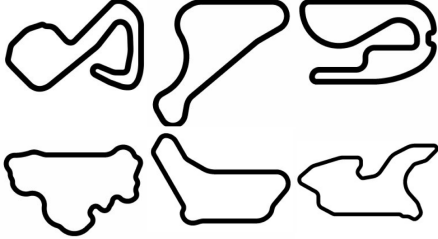


Figure 6: Shape of the 6 tracks in TORCS simulator from which virtual data is collected.

becomes

$$\mathcal{L}_d(D, G) = \mathbb{E}_{\mathbf{x}^v} [D(\mathbf{x}^v; \theta_D)^2] + \quad (9)$$

$$\mathbb{E}_{\mathbf{x}^r} [(1 - D(G(\mathbf{x}^r; \theta_G); \theta_D))^2], \quad (10)$$

Second, we train the discriminator using a buffer of generated images to alleviate model oscillation [26]. We use a buffer size of 50.

In order to take advantage of the labeled data collected from simulators, we initialize the predictor network with a model that is pretrained on virtual images. We cannot train the network with data from virtual and real datasets simultaneously as they are on different scales and no clear

conversion rule exists. During pretraining, we set batch size to 2000 and learning rate to 0.01.

At each step, we sequentially update θ_G , θ_P and θ_D with respect to the objective functions in 5, 6 and 7. We use a batch size of 60. We set $\alpha_P = 0.0001$ and $\alpha_{GAN} = 0.00001$. In our experiments, we use a cliff function for the schedule of λ . We set $\lambda = 0$ for the first 2 epochs, then increase λ to 1. We train the model for a total of 7 epochs.

After obtaining a real-to-virtual generator for each real domain, we could fix the generator and train a global predictor with all real datasets. We initialize the global predictor with *PilotNet* pretrained on virtual data, and use a learning rate of 0.001 and a batch size of 2000 for training.

4.4. Metrics and baselines

We evaluate the effectiveness of our model in terms of the quality of generated images in the virtual domain and the mean absolute error of steering angle prediction. We compare the performance of DU-drive with the following baselines. To ensure fairness, we use the same architecture for the predictor network as described in section 3.1.

Vanilla end-to-end model (*PilotNet*) Our first baseline is a vanilla end-to-end model, where a real driving image is



Figure 7: Image generation results of conditional GAN. Mode Collapse happens for both background and foreground, and lane markings are not preserved.



Figure 8: Image generation results of CycleGAN. Top row: real source images and generated fake virtual images. Bottom row: virtual source images and generated fake real images.

directly mapped to a steering command. This is essentially the same model (*PilotNet*) as employed by [5].

Finetune from virtual data A straightforward way to do domain adaption is to finetune a model pretrained in the source domain with data in the target domain. We first train a predictor with virtual data only, then finetune it with the real dataset.

CycleGAN CycleGAN [15] is a method to do unpaired image-to-image translation, which could also be applied to transforming real driving images to the virtual domain. It uses one generative adversarial network $G_{X \rightarrow Y}$ to transform image x from domain X to image $G_{X \rightarrow Y}(x)$ in domain Y , and another generative adversarial network $G_{Y \rightarrow X}$ to transform $G_{X \rightarrow Y}(x)$ back to an image $G_{Y \rightarrow X}(G_{X \rightarrow Y}(x))$ in domain X . A cycle consistency loss is employed to ensure that $G_{Y \rightarrow X}(G_{X \rightarrow Y}(x)) = x$.

Conditional GAN A naive implementation of conditional GAN (cGAN) [22] uses a generator G to transform an image x from the real domain to an image $G(x)$ in the virtual domain. A discriminative network D is set up to discriminate $G(x)$ from y sampled from the virtual domain while G tries to fool the discriminator. No additional supervision is provided other than the adversarial objective. We also train a *PilotNet* to predict steering angle from the fake virtual image generated by cGAN.

***PilotNet* joint training** To verify the effectiveness of our domain unification model, we also directly train a *PilotNet*

with two labeled real datasets simultaneously.

4.5. Results and Comparisons

Quantitative Results We compare the performance of steering command prediction for a single real domain of our DU-drive(single) model with plain end-to-end model (*PilotNet*), finetuning from virtual data and conditional GAN without joint training (Table 2). Both DU-drive(single) and finetuning from virtual data performs better than plain end-to-end model, which verifies the effectiveness of introducing labeled virtual data. DU-drive outperforms finetuning by 12%/20% for Comma.ai/Udacity dataset respectively with the same training data and prediction network but different input data representation. This verifies the superiority of transforming complex real images into their canonical representation in the virtual domain for driving command prediction task. Conditional GAN without joint training does not perform well as adversarial objective itself is not enough to ensure the preservation of label.

Qualitative Results Sample virtual images generated by DU-drive (Figure 5) shows that our model can indeed transform real driving images to their canonical representations in the virtual domain. Superfluous details including views beyond the road and lighting conditions are unified into clean grayish grounds. Interestingly, traffics are also removed from the scenes, which is actually reasonable on second thought as we are only predicting steering angle. Es-

Dataset	Model	MAE	SD
Comma.ai	<i>PilotNet</i> [5]	1.208	1.472
	Finetune TORCS	1.203	1.500
	cGAN [22]	1.215	1.405
	<i>PilotNet</i> joint training	5.988	11.670
	DU-Drive(single)	1.061	1.319
	DU-Drive(unified)	1.079	1.270
Udacity	<i>PilotNet</i> [5]	6.018	7.613
	Finetune TORCS	5.808	7.721
	cGAN [22]	5.921	6.896
	<i>PilotNet</i> joint training	15.040	27.636
	DU-Drive(single)	4.558	5.356
	DU-Drive(unified)	4.521	5.558

Table 2: Steering angle prediction performance in terms of mean absolute error (MAE) and its standard deviation (SD). DU-drive outperforms all baseline methods.

entially, only lane markings are preserved, which is indeed the most important, if not the only critical information for steering angle prediction.

4.6. Effectiveness of Domain Unification

A critical advantage of our model is that data collected from different sources could be unified to the same virtual domain. As shown in Figure 5, images from Comma.ai dataset (upper row) and those from Udacity dataset (lower row) are transformed into their canonical representations in a unified virtual domain, whose superiority is directly reflected in the performance of steering angle prediction task. As shown in Table 2, directly training a network with data from two real domains together will lead to results much worse than training each one separately due to domain shift. However, with DU-drive(unified), a single network could process data from multiple real domains with comparable results with DU-drive(single). Moreover, DU-drive separates the transformation and prediction process, and a generator could be independently trained for a new real dataset. This demonstrates the superiority of our model at unifying data collected from different source domains into their canonical representations in the virtual domain.

4.7. Discussion

Selective prevention of mode collapse Mode collapse is a common pitfall for generative adversarial networks. Due to the lack of additional supervision from joint training with the predictor network, conditional GAN easily suffers from unstable training and mode collapse for both the background and the foreground (Figure 7). With our novel joint training of steering angle prediction and real-to-virtual transformation, while mode collapse for the background still occurs, mode collapse for driving critical information (*i.e.* lane markings) is effectively prevented.

Comparison with CycleGAN Although CycleGAN

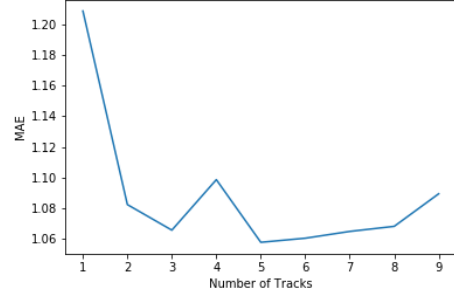


Figure 9: Change of mean absolute error of prediction task as the diversity of virtual dataset increases.

seems to do better at recovering details (Figure 8), which could be important in many generation tasks, the additional details that are unrelated to steering angle prediction does not help much for our task. It also comes at a cost of high memory usage, which could make joint training with the predictor difficult. Moreover, since real images are more complex than virtual images, the generated fake real images often include lots of undesired hallucinated details, which justifies our motivation to go the other way around.

Effect of virtual data diversity We study the effect of the diversity of the virtual dataset on model performance. We repeat our experiments with virtual datasets captured on different numbers of unique tracks (from one to nine) and report the prediction MAE. Figure 9 shows that the performance of the prediction task improves as the diversity of virtual dataset increases up to a certain point. Furthermore diversity does not help much in our experiments, which we believe is due to the limited variance in both rendered images and highway driving scenes, which is inherent to the simulator and the application scenario. Additional diversity that goes beyond the capacity of our current simulator could potentially improve the performance and expand the scope of application of our method.

5. Conclusion

We propose an unsupervised real to virtual domain unification model for highway driving, or DU-drive, that employs a conditional generative adversarial network to transform driving images in a real domain to their canonical representations in the virtual domain, from which vehicle control commands are predicted. In the case where there are multiple real datasets, a real-to-virtual generator could be independently trained for each real domain and a global predictor could be trained with data from multiple real domains. Qualitative experiment results show that our model can effectively transform real images to the virtual domain while only keeping the minimal sufficient information, and quantitative results verifies that such canonical representation can indeed eliminate domain shift and boost the performance of control command prediction task.

References

- [1] Autonomous off-road vehicle control using end-to-end learning. <http://net-scale.com/doc/net-scale-dave-report.pdf>. Accessed: 2017-10-20. **2**
- [2] Udacity self-driving-car challenge dataset. <https://github.com/udacity/self-driving-car/tree/master/datasets>. Accessed: 2017-10-20. **5**
- [3] M. Abadi, A. Agarwal, P. Barham, E. Brevdo, Z. Chen, C. Citro, G. S. Corrado, A. Davis, J. Dean, M. Devin, et al. Tensorflow: Large-scale machine learning on heterogeneous distributed systems. *arXiv preprint arXiv:1603.04467*, 2016. **5**
- [4] S. Bickel, M. Brückner, and T. Scheffer. Discriminative learning for differing training and test distributions. In *Proceedings of the 24th international conference on Machine learning*, pages 81–88. ACM, 2007. **2**
- [5] M. Bojarski, D. Del Testa, D. Dworakowski, B. Firner, B. Flepp, P. Goyal, L. D. Jackel, M. Monfort, U. Muller, J. Zhang, et al. End to end learning for self-driving cars. *arXiv preprint arXiv:1604.07316*, 2016. **1, 2, 4, 5, 7, 8**
- [6] M. Bojarski, P. Yeres, A. Choromanska, K. Choromanski, B. Firner, L. Jackel, and U. Muller. Explaining how a deep neural network trained with end-to-end learning steers a car. *arXiv preprint arXiv:1704.07911*, 2017. **2, 4**
- [7] K. Bousmalis, N. Silberman, D. Dohan, D. Erhan, and D. Krishnan. Unsupervised pixel-level domain adaptation with generative adversarial networks. In *Proceedings of the IEEE conference on computer vision and pattern recognition*, pages 3722–3731, 2017. **2, 3, 4**
- [8] C. Chen, A. Seff, A. Kornhauser, and J. Xiao. Deepdriving: Learning affordance for direct perception in autonomous driving. In *Proceedings of the IEEE International Conference on Computer Vision*, pages 2722–2730, 2015. **1, 2, 5**
- [9] E. D. Dickmanns and V. Graefe. Dynamic monocular machine vision. *Machine vision and applications*, 1(4):223–240, 1988. **1, 2**
- [10] E. D. Dickmanns, B. Mysliwetz, and T. Christians. An integrated spatio-temporal approach to automatic visual guidance of autonomous vehicles. *IEEE Transactions on Systems, Man, and Cybernetics*, 20(6):1273–1284, 1990. **1, 2**
- [11] Y. Ganin and V. Lempitsky. Unsupervised domain adaptation by backpropagation. In *International Conference on Machine Learning*, pages 1180–1189, 2015. **2**
- [12] I. Goodfellow, J. Pouget-Abadie, M. Mirza, B. Xu, D. Warde-Farley, S. Ozair, A. Courville, and Y. Bengio. Generative adversarial nets. In *Advances in neural information processing systems*, pages 2672–2680, 2014. **2**
- [13] K. He, X. Zhang, S. Ren, and J. Sun. Deep residual learning for image recognition. In *Proceedings of the IEEE conference on computer vision and pattern recognition*, pages 770–778, 2016.
- [14] B. Huval, T. Wang, S. Tandon, J. Kiske, W. Song, J. Pazhayampallil, M. Andriluka, P. Rajpurkar, T. Migimatsu, R. Cheng-Yue, et al. An empirical evaluation of deep learning on highway driving. *arXiv preprint arXiv:1504.01716*, 2015. **2**
- [15] P. Isola, J.-Y. Zhu, T. Zhou, and A. A. Efros. Image-to-image translation with conditional adversarial networks. In *The IEEE Conference on Computer Vision and Pattern Recognition (CVPR)*, July 2017. **3, 4, 7**
- [16] J. Janai, F. Güney, A. Behl, and A. Geiger. Computer vision for autonomous vehicles: Problems, datasets and state-of-the-art. *arXiv preprint arXiv:1704.05519*, 2017. **2**
- [17] J. Johnson, A. Alahi, and L. Fei-Fei. Perceptual losses for real-time style transfer and super-resolution. In *European Conference on Computer Vision*, pages 694–711. Springer, 2016. **3, 4**
- [18] J. Kim and J. Canny. Interpretable learning for self-driving cars by visualizing causal attention. In *The IEEE International Conference on Computer Vision (ICCV)*, Oct 2017. **1, 2, 5**
- [19] D. Kingma and J. Ba. Adam: A method for stochastic optimization. In *International Conference on Learning Representations*, 2015. **5**
- [20] M.-Y. Liu and O. Tuzel. Coupled generative adversarial networks. In *Advances in neural information processing systems*, pages 469–477, 2016. **2**
- [21] X. Mao, Q. Li, H. Xie, R. Y. Lau, and Z. Wang. Least squares generative adversarial networks. In *Proceedings of the IEEE International Conference on Computer Vision*, 2017. **5**
- [22] M. Mirza and S. Osindero. Conditional generative adversarial nets. *arXiv preprint arXiv:1411.1784*, 2014. **3, 7, 8**
- [23] V. M. Patel, R. Gopalan, R. Li, and R. Chellappa. Visual domain adaptation: A survey of recent advances. *IEEE signal processing magazine*, 32(3):53–69, 2015. **2**
- [24] D. A. Pomerleau. Alvin: An autonomous land vehicle in a neural network. In *Advances in neural information processing systems*, pages 305–313, 1989. **1, 2**
- [25] E. Santana and G. Hotz. Learning a driving simulator. *arXiv preprint arXiv:1608.01230*, 2016. **5**
- [26] A. Shrivastava, T. Pfister, O. Tuzel, J. Susskind, W. Wang, and R. Webb. Learning from simulated and unsupervised images through adversarial training. In *The IEEE Conference on Computer Vision and Pattern Recognition (CVPR)*, July 2017. **3, 4, 6**
- [27] C. Thorpe, M. H. Hebert, T. Kanade, and S. A. Shafer. Vision and navigation for the carnegie-mellon navlab. *IEEE Transactions on Pattern Analysis and Machine Intelligence*, 10(3):362–373, 1988. **1, 2**
- [28] J. Tobin, R. Fong, A. Ray, J. Schneider, W. Zaremba, and P. Abbeel. Domain randomization for transferring deep neural networks from simulation to the real world. *arXiv preprint arXiv:1703.06907*, 2017. **3**
- [29] A. Torralba and A. A. Efros. Unbiased look at dataset bias. In *Computer Vision and Pattern Recognition (CVPR)*, 2011 IEEE Conference on, pages 1521–1528. IEEE, 2011. **2**
- [30] E. Tzeng, J. Hoffman, T. Darrell, and K. Saenko. Simultaneous deep transfer across domains and tasks. In *Proceedings of the IEEE International Conference on Computer Vision*, pages 4068–4076, 2015. **2**
- [31] E. Tzeng, J. Hoffman, K. Saenko, and T. Darrell. Adversarial discriminative domain adaptation. In *Computer Vision and Pattern Recognition (CVPR)*, 2017 IEEE Conference on, pages 7167–7176. IEEE, 2017. **2**

- [32] B. Wymann, E. Espié, C. Guionneau, C. Dimitrakakis, R. Coulom, and A. Sumner. Torcs, the open racing car simulator. *Software available at <http://torcs.sourceforge.net>*, 2000. 5
- [33] H. Xu, Y. Gao, F. Yu, and T. Darrell. End-to-end learning of driving models from large-scale video datasets. In *Proceedings of the IEEE conference on computer vision and pattern recognition*, pages 2174–2182, 2017. 1, 2
- [34] Y. You, X. Pan, Z. Wang, and C. Lu. Virtual to real reinforcement learning for autonomous driving. *arXiv preprint [arXiv:1704.03952](https://arxiv.org/abs/1704.03952)*, 2017. 2, 3
- [35] J.-Y. Zhu, T. Park, P. Isola, and A. A. Efros. Unpaired image-to-image translation using cycle-consistent adversarial networks. In *The IEEE International Conference on Computer Vision (ICCV)*, Oct 2017. 3, 5